

1 **Satellite-Based Assessment of Hailstorm Affected Potato Crop for Insurance Purpose**

2 Karun Kumar Choudhary<sup>a\*</sup>, Abhishek Chakraborty<sup>a</sup>, CS Murthy<sup>a</sup> and MK Poddar<sup>b</sup>

3 *<sup>a</sup>Agricultural Sciences and Applications Group, National Remote Sensing Centre, Indian*  
4 *Space Research Organization, Balanagar, Hyderabad, India*

5 *<sup>b</sup>Agriculture Insurance Company of India Limited., East Kidwai Nagar, New Delhi, India*

6

7 \*karunkc@gmail.com

8  <https://orcid.org/0000-0002-5877-3546>

9

10

11

12

13

14

15

16

17

18

19

20

21

22

23

24

25

26

27

28

29

30

# 31 **Satellite-Based Assessment of Hailstorm Affected Potato Crop for Insurance Purpose**

## 32 **Abstract**

33 Assessing the extent of hailstorm affected crop is one of the thrust areas for quantifying  
34 mid-season adversaries under crop insurance values chain. This study evaluated the pre-  
35 and post-hailstorm responses on spectral bands and vegetation indices derived from  
36 Sentinel-2 data for assessing the severity class of the affected potato crop. The potato  
37 crop was mapped using pre-event satellite data with overall accuracy of 88% ( $\kappa=0.82$ ).  
38 Pair-wise Games-Howell t-test showed significant differences among the post-hailstorm  
39 potato severity classes in Red, Near Infrared & Short-wave Infra-red (SWIR) bands and  
40 Normalized vegetation indices. Percentage change (from pre- to post-event) in band  
41 reflectance and vegetation indices showed a better sensitivity in differentiating damage  
42 severity. Differential behaviour of SWIR-1 (Band-11) and SWIR-2 (Band-12) were  
43 observed within severely affected potato crop under dry and wet soil conditions. Decision  
44 matrix based on percentage change in Normalized difference Vegetation Index ( $\Delta$ NDVI)  
45 and Normalized difference Tillage Index ( $\Delta$ NDVI) could able to capture the damage  
46 severity classes with an overall accuracy of 86.7%. Higher proportion of affected area  
47 were found to be associated with larger percentage of Potato yield reduction based on  
48 measured yield data at Insurance unit level. The proposed methodology could be adopted  
49 for operational assessment of the impact of hailstorm events on crops.

50

51 **Keywords:** *Solanum*; NDVI; NDTI; hailstorm; damage; crop insurance

## 52 **1 Introduction**

53 Since past decades, there has been unprecedented increase in the extreme weather events in the  
54 Indian subcontinent, which has made the agriculture more vulnerable and riskier (De et al. 2005;  
55 Mohanty, 2020). Hailstorms coupled with unseasonal rainfall is one of such weather extremes  
56 mostly observed in the northern to central Indian region during pre-monsoon season (February  
57 to April) and causes damage over large area of cultivated winter (*rabi*) crops especially wheat,  
58 potato, mustard, gram etc. (Rao et al. 2014). Indian states of Himachal Pradesh, Uttar Pradesh,  
59 Punjab, Haryana, Rajasthan, West Bengal, Madhya Pradesh, Maharashtra, Telangana and

60 Andhra Pradesh are considered to be more vulnerable to hailstorms as the annual probability of  
61 occurrence of hailstorm in these areas is more than 50% and also showed significant surge in  
62 past years (Chattopadhyay et al. 2017). Hailstorms are sporadic and localized phenomena,  
63 difficult to forecast because of limited radar networks, resulting in unavoidable crop losses (Bal  
64 et al. 2014). Widespread damages of *rabi* crops due to hailstorms in 2014 and 2015 are well  
65 known recent examples (Kulkarni et al. 2015; Bal et al. 2017).

66 The crop insurance is one of the efficient mechanisms to cope with the hailstorm damage  
67 by providing compensation to the farmers as par the yield reduction. In India crop insurance  
68 mechanism is based on the area-yield approach. But in case of the hailstorm damage, insurance  
69 claims can be raised both based on area-yield approach as well as individual farmer level  
70 (PMFBY 2016). Hence, it is very essential to assess the spatial extent and the intensity of the  
71 hailstorm damage in near-real time to initiate the compensation, relief or remedial processes.  
72 Traditional ground survey-based damage area assessment is laborious, time consuming, cost  
73 ineffective and subjected to individual bias, particularly over a large areal extent and relatively  
74 inaccessible locations (Bentley et al. 2002). Alternatively, space-based input can help in  
75 assessing and quantifying the damaged area through the synoptic, repetitive and multi-band  
76 information from satellites platform and in turn would assist informed decision making (Apan  
77 et al. 2005).

78 Remote sensing (RS) has been used since decades for crop discrimination, crop health  
79 assessment and crop damages due to different biotic and abiotic agents (Moran et al. 1997).  
80 But, limited studies had been found specific to RS based assessment of hailstorm damage. One  
81 of the earliest RS-based studies for quantifying the crop losses by hail was done in central  
82 Illinois using infrared and standard colour aerial photographs (Changnon and Baron 1971).  
83 Thereafter, series of studies had been conducted to showcase the potential of infrared aerial  
84 photographs to detect crop-hail damage (Towery et al. 1975; Towery 1980) to support insurance

85 activities. Erickson et al. (2004) used multispectral and hyperspectral airborne data and reported  
86 the importance of NIR and red bands in assessing the defoliation in maize. Subsequently many  
87 researchers had started using satellite platform for crop-hail damage assessments. Gillis et al.  
88 (1990) used Landsat TM data to map damaged area in operational salvage harvest due to hail.  
89 Klimowski et al. (1998) observed the hailstorm damage from the geostationary satellite GOES-  
90 8 using imageries in visible region. Peters et al. (2000) utilized Landsat TM multispectral data  
91 for detection of hail damaged area of corn and soybean. Normalized Difference Vegetation  
92 Index (NDVI) derived from Near Infra-Red (NIR) and Red band reflectance is most widely  
93 used index for hailstorm damage assessment. Most of the hail damage related studies were  
94 based on pre- and post-event NDVI changes (Bentley et al. 2002; Parker et al. 2005; Gallo et  
95 al. 2012; Zhao et al. 2012). These researchers have reported a significant decrease of post-event  
96 NDVI (in comparison to pre-event NDVI) over the hailstorm damaged vegetation which was  
97 completely destroyed, but none of them have commented on the partially damaged crops. In  
98 India, limited studies have been conducted to assess the hailstorm damage of crops such as  
99 wheat (Ray et al. 2016; Singh et al. 2017) and other mixed crops (Prabhakar et al. 2019) using  
100 multispectral satellite data. Singh et al. (2017) has proposed a Percentage Difference Index  
101 (PDI), which accounts for the changes in NDVI between normal and current (hail storm  
102 affected) years. Such approach is limited over areas with stable cropping pattern where year to  
103 year variations of crop calendar is minimal. Space based assessment of hailstorm damage of  
104 potato crop is rare. Zhou et al. (2016) used airborne multispectral data and concluded that Green  
105 NDVI, NDVI and soil-adjusted NDVI can well assess the hail damage at early stages of potato  
106 crop. The present study is the maiden attempt to assess potato crop damaged due to hailstorm  
107 over India using satellite observations and ground informations.

108         Potato (*Solanum tuberosum* L.), also known as “The king of vegetables”, is the third  
109 most consumed crop after rice and wheat (Nagar et al. 2019). Indian ranks second in potato

110 production in the world. The area under potato cultivation in India was 2.1 m ha, which give  
111 rise production of 52.59 m tons in 2018 (DACFW 2020). Hence, potato plays a very important  
112 role in the food and nutritional security of rural India, but the crop is subjected to damage due  
113 to hailstorm and unseasonal rainfall periodically (Tiwari et al. 2021). Hailstorms affect the  
114 standing potato crop in two ways. The beating action of the solid hails break the foliage,  
115 lacerates the stem, disrupt the ridge and furrow structure of the field and partially expose the  
116 tuber. The post-hail rainfall causes stagnation of water which leads to the rotting of tuber and  
117 secondary infection. The occurrences of hailstorms in India mostly coincide with the  
118 tuberization phase of the crop with high above-ground green foliage and cause significant yield  
119 reduction (Irigoyen et al. 2011; Jalali 2013). Hence, an objective assessment of the hailstorm  
120 damage of potato crop in near-real time using space-based input is need of the hour to support  
121 insurance claims.

122 As discussed earlier, space-based studies to assess the hailstorm related crop damage  
123 have predominantly used NDVI (which represents the crop vigour) as an indicator. These  
124 studies did not include different short-wave infrared (SWIR) bands which are sensitive to  
125 exposed soil, surface wetness as well as non-photosynthetic vegetation (NPV) (Quemada and  
126 Daughtry 2016). With the advent of medium resolution (10-20 m) satellite data like Sentinel-2  
127 with wide swath (~300 km), 5 days temporal receptivity, and bands ranging from VNIR to  
128 SWIR, the observational capacity has increased tremendously especially for *rabi* season crop  
129 like potato (Drusch et al. 2012). Keeping the above-mentioned points in mind, the present study  
130 is mainly focussed on identifying spectral bands/vegetation indices that can discriminate  
131 different levels of hailstorm affected potato crops. Further, the study also proposes an operation  
132 methodology towards objective assessment of the hailstorm affected potato crop which could  
133 represent yield loss at insurance unit level.

## 134 **2 Material and Methods**

### 135 **2.1 Study area**

136 West Bengal experienced a series of hailstorm events accompanied with rains on 25<sup>th</sup>, 27<sup>th</sup> and  
137 28<sup>th</sup> Feb 2019 (NIE 2019; Weather 2019). All the southern districts of West Bengal were more  
138 or less affected by it but major damage of potato crops was reported from Hooghly and West  
139 Medinipur districts as per the information received from National Insurance Company Limited  
140 (NIC), Kolkata. Hence, these two districts were selected for the present study (Fig 1). The study  
141 area lies between 21.76° N to 23.22° N latitude and 88.51° E to 87.05° E longitude with mean  
142 elevation of 25 m and mean annual rainfall of 1500 mm (ICAR 2017). The area falls under  
143 agro-ecological region 15 i.e., Bengal and Assam plains with hot sub-humid to humid eco-sub  
144 region. The soil is alluvium with loam to clay loam texture. The geographical area of Hooghly  
145 and West Medinipur are 3.13 and 9.28 lakh ha with net sown area of 2.12 and 5.17 lakh ha  
146 respectively (Matirkatha 2016). As per the horticultural statistics of 2016 the potato area of  
147 Hooghly and West Medinipur districts were 1.11 & 0.86 lakh ha with production of 14.13 &  
148 15.48 lakh tons respectively (Glance 2018).

149 [Insert Figure 1](#)

### 150 **2.2 Data sets**

#### 151 **2.2.1 Ground data**

152 Pre-event ground observations related to the crop type, crop stages, geo-locations etc. were  
153 collected during 14-19 February as a part of ongoing FASAL programme (Parihar and Oza  
154 2006) and were further used for classification of the crops in the study area (Fig 2a). Post-event  
155 field survey was conducted during 01-05 March 2019 to assess the damages to the crops. The  
156 severity of damage to potato crop was recorded through visual inspection and categorized as

157 “Unaffected” (<20% damage of the canopy foliage), “Moderately-affected” (20-50% damage  
158 of the canopy foliage) and “Severely-affected” (> 50% damage of the canopy foliage). The  
159 locations of the field data points of the different classes of potato crop affected by the hailstorm  
160 are presented in Fig. 2b. Soil moisture variations were also observed in “Severely affected”  
161 class as “Dry” and “Wet”. Total 54 points were collected over “Unaffected” class, whereas 48  
162 and 61 points were collected over “Moderately-affected” and “Severely-affected” categories  
163 respectively. Each field data points were converted to a polygon by considering minimum 3x3  
164 homogeneous pixels and further used for statistics generation. Out of the total points collected  
165 over the study area, nearly 75% of the points were used for developing the methodology and  
166 the remaining points were used for validation.

167 [Insert Figure 2](#)

### 168 *2.2.2 Satellite data*

169 Cloud free Sentinel-2 data of two-time epochs i.e., pre-event (19<sup>th</sup> February 2019) and post-  
170 event (01<sup>st</sup> March 2019) were used in the present study (Fig 2). The surface reflectance product  
171 (L2A) of Sentinel-2 were band composited, stacked, exported and downloaded through earth  
172 engine cloud computing environment in java script (Gorelick et al. 2017). Subsequent  
173 processing of the Sentinel-2 data comprising of six bands (Table 1) were done in ERDAS  
174 IMAGINE 16.1 and ArcGIS Desktop 10.6.

175 [Insert Table 1](#)

176

### 177 *2.3 Mapping potato crop*

178 Training classes were generated using pre-event ground data (during 14-19 Feb, 2019) and  
179 spectral signatures were generated using six bands of sentinel-2 corresponding to 19<sup>th</sup> February.  
180 Training classes comprised of potato, rice, and other crops (chilli, vegetables and scrubs). The

181 classification was done over the agricultural area only, excluding other non-agricultural areas  
182 using 1:50000 land use land cover map (NRSC 2014). Major growing crops were classified  
183 using Spectral Angle Mapper (SAM) algorithm as described by Kumar et al. (2015) and Zhou  
184 et al. (2015). The classification accuracy of the crop map was evaluated using confusion  
185 matrices.

#### 186 *2.4 Analysis of variance between severity classes*

187 Band specific reflectance statistics of Sentinel-2 data (both 19<sup>th</sup> February and 1 March, 2019)  
188 over the different categories of potato crop affected due to hailstorm were generated using post  
189 event ground truth data points as mentioned in section 2.2.1. These statistics were further  
190 analysed to assess the changes in reflectance between the pre- and post-event vis-a-vis the  
191 damage severity. The percentage change in reflectance ( $\Delta B$ ) of each band is calculated as per  
192 the equation 1.

$$193 \quad \Delta B = \frac{B_{post} - B_{pre}}{B_{pre}} \times 100 \quad \text{Equation 1}$$

194 Where,  $B_{pre}$  is the reflectance of a band at pre-event (19<sup>th</sup> February, 2019) and  $B_{post}$  is the  
195 reflectance of a band at post-events (1<sup>st</sup> March, 2019)

196 Four vegetation indices were calculated using different spectral reflectance (Red, NIR,  
197 SWIR) of Sentinel-2 data (Table 2). These are NDVI, Normalized difference Water Index  
198 (NDWI), Land Surface Water Index (LSWI), Normalized Difference Tillage Index (NDTI).  
199 The band combinations used to generate these indices along with their sensitivity towards  
200 different biophysical properties are mentioned in Table-2.

201 [Insert Table 2](#)

202 The percentage change in VIs ( $\Delta VI$ ) from pre- to post-event is calculated using equation 2:

$$\Delta VI = \frac{VI_{post} - VI_{pre}}{VI_{pre}} \times 100 \quad \text{Equation 2}$$

Where,  $VI_{pre}$  is the VI at pre-event (19<sup>th</sup> February, 2019) and  $VI_{post}$  is the VI at post-events (1<sup>st</sup> March, 2019). Likewise,  $\Delta NDVI$ ,  $\Delta NDWI$ ,  $\Delta LSWI$  and  $\Delta NDTI$  were computed for the three categories of crop damage due to the hailstorm. The  $\Delta B$  and  $\Delta VI$  were further analysed statistically towards their sensitivity to explain the severity of the damage and further compared pair-wise using Games-Howell test (Games and Howell 1976).

### 2.5 Yield reduction due to hail storm damage

Crop cutting experiment (CCE) data of potato at Gram Panchayet (GP) level (administrative unit for crop insurance) for the year 2019 and also for the past five years were analysed. Average yield of the potato crop was calculated by the mean value of last five years of CCE data. Subsequently, percentage yield deviation ( $\Delta Y$ ) was computed using the equation 3:

$$\Delta Y = \frac{Yield_{2019} - Yield_{Average}}{Yield_{Average}} \times 100 \quad \text{Equation 3}$$

Where,  $Yield_{2019}$  is GP averaged potato yield ( $\text{ton ha}^{-1}$ ) in 2019 and  $Yield_{Average}$  is historical five-year average yield ( $\text{ton ha}^{-1}$ ) of GP. Percent yield deviation data were divided into five yield reduction classes and compared with  $\Delta B$  and  $\Delta VI$ .

## 3 Results and Discussions

### 3.1 Hailstorm and damage to potato crop

Hooghly and West Medinipur districts of West Bengal state were exposed to hailstorm during 25-28 February, 2019 accompanied with moderate to heavy rainfall causing significant damage to potato crop from falling hails and water stagnation. The daily India Meteorological Department (IMD) gridded rainfall data showed high intensity rainfall over the Hooghly and

224 West Medinipur districts (Fig. 3). The cumulative rainfall between 25-28 February was found  
225 to be more than 100 mm in the parts of districts.

226 [Insert Figure 3](#)

227 As per the ground truth data collected, there were two prominent standing crops over  
228 the two districts i.e., potato and rice. The rice fields were found to be unaffected by the  
229 hailstorm-rainfall as they were in the early tillering stage and grown in flooded condition. On  
230 the other hand, hails had caused considerable damage to the above ground succulent foliage of  
231 the potato crop by breaking/ lacerating it and exposing the below canopy soil. The ridge and  
232 furrow structure of the potato field were also disturbed and the potato tubers were exposed  
233 partly. The water stagnation due to heavy rainfall further disrupt the soil aeration, causing  
234 yellowing of the leaf, rotting of the potato tuber and forced-harvesting in some places.

235 Fig. 4 showed varying degree severity of damage of the potato crop due to the hailstorm  
236 event. The unaffected crops were found have high in leaf greenness and leaf moisture, high  
237 ground cover (>80%) and less exposure to the soil. Whereas, moderately affected crops were  
238 relatively low in leaf greenness and leaf moisture, canopy cover was found to be moderate (50-  
239 80%). The severely affected crop appeared to be yellowish or dried with less canopy cover  
240 (<50%), soil is completely exposed showing the ridge-furrow structure of the potato field.

241 [Insert Figure 4](#)

### 242 ***3.2 Spatial distribution of potato crop***

243 The potato crop map generated using pre-event (19<sup>th</sup> February, 2019) Sentinel-2 data is shown  
244 in Fig 5(a). The potato crop was found to be well separated from the other competing crops like  
245 rice and vegetables due its typical growth stage having luxurious green foliage and row  
246 structure. Hence, potato crop was successfully classified with producer's accuracy of 94.9%  
247 and user's accuracy of 87.5%. The overall accuracy was found to 88% be with kappa coefficient  
248 of 0.82. Potato crop was found to be mostly concentrated in the south-western part of the

249 Hooghly district and north-eastern part of the West Medinipur district. Tarakeshwar, Pursura  
250 and Jangipara blocks in Hooghly; and Chandrokona, Goghat and Keshpur blocks in West  
251 Medinipur district were the dominant blocks having large area under potato crop. GP-wise  
252 potato area statistics showed that out of total 248 GPs in Hooghly district, 154 GPs were having  
253 more than 100 ha under potato cultivation; while in West Medinipur district 77 GPs fulfilled  
254 such criterion out of 305 GPs (Fig 5b). GPs with large area under potato cultivation (more than  
255 500 ha) were found to be 72 in Hooghly district and 26 in West Medinipur district.

256 [Insert Figure 5](#)

### 258 ***3.3 Spectral response to hailstorm damage***

259 The surface reflectance (pre-event: 19<sup>th</sup> February and post-event: 1 March) of six selected bands  
260 of Sentinel-2 over the different categories of damage severity of potato crop are shown in Fig.6.  
261 It is evident from the graph that there exists a large difference between the NIR (B8) reflectance  
262 of pre- and post-event for hailstorm affected potato crop. The magnitude of difference increases  
263 with the degree of severity. The mean reflectance of NIR band in “unaffected” crop was 30%  
264 with standard deviation (SD) of 3%, while for “moderately affected” and “severely affected”  
265 crop it was found to be  $25\pm 2.5\%$  and  $20\pm 4.6\%$  respectively. Marginal response was also  
266 observed over B4 (Red), B11 (SWIR1) and B12 (SWIR2) bands.

267 [Insert Figure 6](#)

268 To investigate further, four bands (B4, B8, B11 and B12) were selected and the data distribution  
269 of these bands during pre- and post-event over the different severity classes were presented in  
270 violin-plots (Fig 7). The violin-plot shows the probability density of the data at different values  
271 smoothed by a kernel density estimator. Hence, the width of the plot represents the density  
272 of the data value and the tapering nature shows the distribution of the data. It is observed that

273 irrespective of the bands, the data distribution of band-reflectance at pre-event remains similar  
274 over the different severity classes. It is further verified by Post-hoc Games-Howell tests  
275 showing no significant difference among them. Such observation confirms that there were no  
276 significant differences in biophysical characteristics of potato crop in term of its vigour,  
277 greenness, wetness and canopy cover before the hailstorm took place. Hailstorm cause  
278 substantial defoliation of potato crop (Zhou et al. 2016) and same observations were also  
279 reported in many other crops (Changnon1971; Chandler et al. 2003). The intensity of the  
280 damage off course depends on the kinetic energy or the size of the hails. But, no such data on  
281 the size of the hail is available over the study site due to lack of hailpads networks. Nevertheless,  
282 varying degree of damages of the potato canopy was observed during the field visit as  
283 mentioned in section 3.1. The rainfall further caused wetness differences depending on the  
284 drainage capacity of the soil. The changes in the canopy cover and surface wetness are well  
285 reflected by the change in shape and position of the violin plots of the post-event observations.  
286 There have been substantial changes either in the central tendency (mean) or the dispersion  
287 (spread or shape) of the violin plots of the post-event vis-a-vis the pre-event observations  
288 irrespective of the bands. The defoliation of the potato canopy cause yellowing of the crop and  
289 substantial reduction in the chlorophyll content. The red band (B4) being a chlorophyll  
290 absorption band, the mean of the post-event red-reflectance over the unaffected crop was found  
291 be significantly different from the affected one (moderately or severely). But the post-event  
292 red-reflectance was not found to be significantly different between “moderately affected” and  
293 “severely affected” crop. On the other hand, the NIR (B8) region of the spectral band is sensitive  
294 to the leaf internal or mesophyll structure. The defoliation causes destruction of the leaf internal  
295 structure depending on the severity of the damage. Hence, statistically significant differences  
296 were observed between the mean of post-event NIR-reflectance between “unaffected” and  
297 “moderately affected”, “unaffected” and “severely affected”, “moderately affected” and

298 “severely affected” crop. The SWIR-1 (B11) and SWIR-2 (B12) bands were sensitive to the  
299 surface wetness (Bidgoli et al. 2020). The surface wetness is attributed both by the leaf and soil  
300 moisture. The defoliation caused by the hailstorm substantially reduces the leaf wetness, but  
301 the associated rainfall led to the increase in soil moisture. Hence, the combined effect of both  
302 has been captured by the SWIR bands. Further, SWIR2 band (2.1  $\mu\text{m}$ ) is also sensitive to the  
303 fractional vegetation cover as it is close to the cellulose absorption band (Quemada and  
304 Daughtry 2016). The mean of post-event SWIR1-reflectance showed significant difference  
305 between “unaffected” and “severely affected”, “moderately affected” and “severely affected”  
306 crop. No significant difference of post-event SWIR1-reflectance was observed between  
307 “unaffected” and “moderately affected” crop. On the other hand, post-event SWIR2-reflectance  
308 was found to be significantly different for “unaffected” and “moderately affected” crop only. It  
309 is important to mention here that the dispersion of post-event SWIRs reflectance is very high  
310 over the severely affected potato crop. It signifies large variations of the surface wetness and  
311 fractional vegetation cover of the severely affected potato crop. In nutshell, it could be  
312 concluded that only post-event NIR-reflectance was found to have statistically significant  
313 differences between the different categories of damage severities of potato crop. But the NIR  
314 reflectance only addresses the changes in the crop vigour or the leaf internal structure. The  
315 greenness and surface wetness of the crop are mainly addressed by the Red and SWIR  
316 reflectance. As per Fig. 7, Red and SWIR reflectance could partially discriminate the different  
317 damage severity classes of the potato crop. Hence, an effort is made to combine these bands to  
318 accommodate their sensitivity towards assessing the different damage classes of the potato crop.

319

[Insert Figure 7](#)

### 320 ***3.4 Response on vegetation indices***

321 Converting reflectance of different bands into a normalized index is an effective approach for

322 improving the sensitivity towards assessing the target features (Xue and Su 2017). Hence, we  
323 generated four normalized indices i.e. NDVI, NDWI, LSWI and NDTI using the selected four  
324 bands as mentioned in the section 3.3. The details of the band combinations are mentioned in  
325 Table 2. The variations of the above-mentioned indices during pre- and post-event conditions  
326 over the different severity classes are presented in box-plots (Fig 8). It is mentioned in the  
327 section 3.3 that all the selected bands (Red, NIR, SWIR-1 and SWIR-2) showed no significant  
328 differences between the damage severity classes at pre-event condition (Fig. 7) signifying  
329 homogeneous potato crop before the occurrence of the hailstorm. Likewise, the indices derived  
330 from these four selected bands did not show any significant differences between the damage  
331 severity classes at pre-event condition (Fig. 8). But distinct variations of data distribution of all  
332 the four indices over the damage severity classes are observed at post-event condition. As a  
333 result, mean of all the four indices showed statistically significant differences between the  
334 severity classes during post-event condition (Fig. 8). It is apt to mention here that among all the  
335 band-reflectance only NIR (i.e. B8) showed such sensitivity towards separating the severity  
336 classes. Hence, there has been a substantial improvement of the sensitivity towards separating  
337 the severity classes by combining the bands into normalized indices.

338 [Insert Figure 8](#)

### 339 ***3.5 Temporal changes in band-reflectance and vegetation indices***

340 To assess the severity of the damage objectively the temporal changes (from pre-event to post  
341 event) of all the selected bands and the vegetation indices were calculated as described in  
342 equation 1 and 2. The mean percentage changes of the band-reflectance ( $\overline{\Delta Red}$ ,  $\overline{\Delta NIR}$ ,  
343  $\overline{\Delta SWIR1}$  and  $\overline{\Delta SWIR2}$ ) and the vegetation indices ( $\overline{\Delta NDVI}$ ,  $\overline{\Delta NDWI}$ ,  $\overline{\Delta LSWI}$ , and  $\overline{\Delta NDTI}$ )  
344 over the different severity classes are presented in Table 3. The variance analysis of these  
345 changes was done and the F-values along with its probability of occurrence by chance are

346 mentioned respectively. Post-hoc Games-Howell tests were performed for separation of the  
347 mean percentage changes and statistically significant differences between the severity classes  
348 are mentioned in Table 3. Out of the four selected band-reflectance, only  $\overline{\Delta NIR}$  showed high  
349 sensitivity and could able to separate different damage severity classes.  $\overline{\Delta Red}$  and  $\overline{\Delta SWIR}$   
350 could separate the “unaffected” and “moderately affected” class significantly. Whereas,  
351  $\overline{\Delta SWIR2}$  could able to separate “moderately affected” and severely affected” classes. The mean  
352 percentage changes of all the vegetation indices i.e.  $\overline{\Delta NDVI}$ ,  $\overline{\Delta NDWI}$ ,  $\overline{\Delta LSWI}$ , and  $\overline{\Delta NDTI}$   
353 were also found to be sensitive. All the metrics of these vegetation indices could able to separate  
354 different damage severity classes of potato crop. Similar sensitivity of the  $\Delta NDVI$  towards the  
355 hailstorm damage of potato crop is reported by Zhou et. Al., 2016. But no such report on the  
356 sensitivity of  $\Delta NDWI$ ,  $\Delta LSWI$  and  $\Delta NDTI$  is found. Importantly,  $\overline{\Delta SWIR1}$  was found to have  
357 negative changes with the increase in the severity of damage meaning more absorption in  
358 SWIR1 band due to net increased in surface wetness. But, the  $\overline{\Delta SWIR2}$  showed positive  
359 changes with the increase of severity of the damage. Hence, in general the reflectance in SWIR2  
360 have increased due to the hailstorm damage of the potato crop.

361 [Insert Table 3](#)

### 362 **3. 6 Variabilities of SWIR-reflectance over the severity classes**

363 As mentioned in section 3.3, there were high variabilities/ dispersions of the post-event SWIR-  
364 reflectance over the “severely affected” potato crop as evident by the shape of the violin plot in  
365 Fig. 7. Further, the differential response of  $\overline{\Delta SWIR1}$  and  $\overline{\Delta SWIR2}$  over the different severity  
366 classes were observed in Table 3. To explain the high variability of SWIR-reflectance, all the  
367 field observations over the “severely affected” potato crop were segregated based on the surface  
368 soil wetness condition i.e. “Severely affected (dry soil)” & “Severely affected (wet soil)”.  
369 Further, all the data points of  $\Delta SWIR1$  and  $\Delta SWIR2$  over the different damage severity classes

370 were put in a scatterplot and shown in Fig.9. The data points pertain to different severity classes  
371 were found to form distinct clusters. As the damage severity increases, the severity-isolines of  
372 the clusters (shown as dotted line in Fig. 9) were found to be frame-shifted. The slopes of the  
373 isolines remained nearly invariant but the offsets were found to be significantly different. The  
374 data point over the “unaffected” potato crop were found to be clustered near to the origin, in  
375 the first and second quadrant of the plot within 10 to -10 of  $\Delta$ SWIR1 and  $\Delta$ SWIR2. On the  
376 other hand, data points over the “moderately affected” crop were found to cluster with -10 to -  
377 20 of  $\Delta$ SWIR1 and 10-20 of  $\Delta$ SWIR2. The data points over the severely affected crop were  
378 found to be widely spread over the first, second and the fourth quadrants of the Fig. 9. The data  
379 points pertain to “severely affected (wet soil)” were typically found in the fourth quadrant of  
380 the plot. Hence, negative values of  $\Delta$ SWIR2 were found over the “severely affected (wet soil)”.  
381 As discussed earlier, the hailstorm affected potato crop in two ways. In first case, the  
382 aboveground succulent vegetation got damaged by hail without appreciable increase in the  
383 background wetness. In the second case, there was appreciable increase in soil wetness in  
384 addition to the foliar damage. High soil wetness condition was predominantly observed over  
385 the “severely affected” crop and may lead to the tuber rot or force harvesting. These  
386 observations of high soil wetness condition were mainly found in the lower ridges of the study  
387 area with limited soil drainage condition. The  $\Delta$ SWIR1 is primarily sensitive to the surface  
388 wetness, hence there had been mainly negative changes of  $\Delta$ SWIR1 due to the hailstorm  
389 damage. The  $\Delta$ SWIR2 is sensitive to fractional vegetation cover (exposed soil surface) and  
390 surface wetness as well. In case of “severely affected (dry soil)” categories, there had been  
391 significant decrease in the fractional vegetation cover and it exposed of the underlying fine  
392 textured dry soil. Thus, it had increased the post-event SWIR2 reflectance and causing positive  
393 change in  $\Delta$ SWIR2. In case of “severely affected (wet soil)” condition the effect of soil wetness  
394 on the SWIR2 reflectance superseded the changes (decrease) in fractional vegetation cover.

395 Hence, we found net absorption in SWIR2 and negative change in  $\Delta$ SWIR2. Such effect is not  
396 observed for SWIR1 reflectance as it is primarily sensitive to the surface wetness. This  
397 differential behaviour of  $\Delta$ SWIR1 and  $\Delta$ SWIR2 in dry fine textured soil is also explained by  
398 Van Deventer et al (1997) using bands of Landsat TM.

399 [Insert Figure 9](#)

### 400 ***3.7 Selecting VIs for affected area assessment***

401 The vegetation indices derived from different band combinations (Red, NIR, SWIR1 and  
402 SWIR2) were found to be suitable for delineating different categories of the damage classes of  
403 potato crop. But there exists redundancy among these vegetation indices as some similar bands  
404 were used to derive it. The guiding principle for remote sensing-based hailstorm damage is  
405 based on the fact that the hailstorm induced changes in the biophysical properties of the crop  
406 can be detected by one or more vegetation indices. The hailstorm induces stress/damage on  
407 potato crop can be addressed using  $\Delta$ NDVI as shown in the present study (Table 3) and also  
408 corroborated by the previous studies (Ray et al. 2016; Prabhakar et al. 2019; Bell et al. 2020).  
409 Hence, NDVI was chosen further for decision matrix generation and it mainly represent the  
410 crop vigour. Post hailstorm stress on potato can also be caused by water stagnation and other  
411 three water indices i.e.  $\Delta$ NDWI,  $\Delta$ LSWI and  $\Delta$ NDTI can address it. To narrow down further, a  
412 correlation analysis was performed within these indices. Correlation matrix of these indices at  
413 pre- and post-event condition is presented in Table-4. Very high correlation was found between  
414 NDWI and LSWI as both indices used NIR and SWIR bands. High correlation is also observed  
415 between NDVI and NDWI/LSWI as NIR-reflectance is common for them. Least correlation  
416 was found between NDVI and NDTI. The band combination used to derive them were also  
417 different. Hence, NDVI and NDTI were further used for decision matrix to delineate different  
418 damage severity classes of potato crop.

419

Insert Table 4

420 Further, scatterplot between  $\Delta\text{NDVI}$  and  $\Delta\text{NDTI}$  over the different damage severity classes is  
421 shown in Fig 10. The plot indicates a clear-cut separation of the three different damage severity  
422 classes of potato crop by forming distinct clusters. The majority points of the “unaffected”  
423 classes were found at the combination of  $\Delta\text{NDVI} \geq -20$  and  $\text{NDTI} \geq -20$ . The “moderately  
424 affected” category was mainly found between  $-20 > \Delta\text{NDVI} \geq -30$  and  $-20 > \Delta\text{NDTI} \geq -30$ .  
425 Whereas, “severely affected” class was found in  $\Delta\text{NDVI} < -30$  and  $\Delta\text{NDTI} < -30$ . These  
426 observations were further used to frame decision matrix.

427

Insert Figure 10

### 428 ***3.8 Decision matrix to map the affected area***

429 Based on the detailed analysis of pre- and post-event Sentinel-2 data and the observations made  
430 thereafter, the following methodology is proposed to assess the potato crop area affected by the  
431 hailstorm (Fig. 11). Assessment of hailstorm damage of a crop requires cloud-free pre-event  
432 and post-event satellite observations along with field data points of the crop, its stages, growing  
433 environment and the intensity of the damage. In the present study, we used 19<sup>th</sup> February, 2019  
434 (pre-event) and 1<sup>st</sup> March, 2019 (post-event) sentinel-2 data to achieve the objectives. The pre-  
435 event satellite data along with ground truth points were used to map the potato crop and further  
436 analysis was done over the potato crop mask only. Two vegetation indices i.e. NDVI and NDTI  
437 were derived using relevant band combinations using pre- and post-event observations (Table  
438 2 and Fig. 11). The percentage change of these vegetation indices between pre- and post-event  
439 i.e.  $\Delta\text{NDVI}$  and  $\Delta\text{NDTI}$  were derived to assess the changes in crop vigour and surface wetness  
440 respectively. Based on the response of  $\Delta\text{NDVI}$  and  $\Delta\text{NDTI}$  over the different damage severity  
441 classes as mentioned in section 3.7 (Fig. 10), these were sliced into different deviation classes  
442 as shown in Fig. 11. These deviation classes of  $\Delta\text{NDVI}$  and  $\Delta\text{NDTI}$  were then combined further

443 using decision matrix as mentioned below and also shown in Fig. 12.

- 444 • If  $\Delta\text{NDVI} \geq -20$  and  $\Delta\text{NDTI} \geq -20$ , the potato crop is “unaffected”.
- 445 • If  $-20 > \Delta\text{NDVI} \geq -30$  and  $-20 > \Delta\text{NDTI} \geq -30$ , the potato crop is “moderately affected”.
- 446 • If  $\Delta\text{NDVI} < -30$  and  $\Delta\text{NDTI} < -30$ , the potato crop is “severely affected”.

447 It is important to mention here that the combination of  $\Delta\text{NDTI} < -30\%$  and  $\Delta\text{NDVI} > -20\%$   
448 were non-existent in the study area as large change in  $\Delta\text{NDTI}$  is not possible without significant  
449 change in vegetation cover i.e.  $\Delta\text{NDVI}$  (Renier et al. 2015). Hence, such categories of classes  
450 were not included in the decision matrix.

451 [Insert Figure 11 and Figure 12](#)

452 Decision matrix was then implemented over the potato pixels to get the different categories of  
453 affected crop over in the study area (Fig 13). Out of the total potato area of 1.21 lakh ha over  
454 both the districts combined, nearly 12% of the area was found to be under “severely affected”  
455 category and 26% of the area was “moderately affected”. The “moderately affected” area was  
456 found to have spatial association with the “severely affected area”. GP-wise percentage of  
457 affected potato area (both severely and moderately) were mapped and presented in Fig.14. The  
458 affected areas were mainly found to be concentrated over the Arambagh, Tarakeshwar &  
459 Khankul blocks of Hooghly district and Chandrakana & Garbeta block of west Medinipur  
460 district. Significant GPs in both the districts were found to be affected by more than 60% of the  
461 affected potato area.

462 [Insert Figure 13 and Figure 14](#)

463 Post-hailstorm field observations (not included to generate criteria for decision matrix) were  
464 used for accuracy assessment of the affected area map (Table 5). The “unaffected” potato crop  
465 was well classified as evident from high producer’s (92.7%) and users (90%) accuracy. The

466 accuracy was found to decrease slightly for other two classes due to omission / commission  
467 errors. The producer accuracies were found to be 75.2% and 88.2 % for “moderately affected”  
468 and “severely affected” classes respectively. On the other hand, the user’s accuracy of  
469 “moderately affected” and “severely affected” classes were found to be 80.1% and 77.3%  
470 respectively. The overall accuracy was found to be 86.7 % with kappa coefficient of 0.81.

471 [Insert Table 4](#)

### 472 ***3.9 Hailstorm affected area vis-à-vis potato yield reduction***

473 To assess the match between the hailstorm affected area and yield reduction of the potato crop,  
474 we calculated the GP-wise yield deviation from normal ( $\Delta Y$ ) using equation 3 as discussed in  
475 section 2.5. GP-wise potato yield deviation of the study year (2019) is presented in Fig 15(a).  
476 The normal (long-term average) potato yield of the study area (Hooghly and West Medinipur)  
477 districts were found to be nearly 20 tones/ha. Large yield deviation was observed due to the  
478 hailstorm in year 2019 and potato yield as low as 10 tones/ha were recorded in some pockets  
479 of the study area. Majority of the GPs in Keshpur, Daspur-1 and Chadrakona-2 blocks of West  
480 Medinipur District; and Khanakul-1&2, Pursura, Jangipara, Dhaniakhali, Singur blocks of  
481 Hooghly district were reported large reduction of potato yield. To assess the match between the  
482 satellite derived affected potato areas and the reported yield reduction from long term average,  
483 the affected (moderate and severely) areas were classified into five classes ( $\leq 10\%$ , 10-20%, 20-  
484 40%, 40-60% and  $>60\%$ ) and the yield reduction at gram panchayat were also made five classes  
485 ( $<20\%$ , 20-40%, 40-60%, 60-80% and  $>80\%$ ). Under each class of the affected area, the  
486 distribution of the GPs having different yield reduction classes were presented in Fig 15b. It  
487 was observed that the GPs with more than 60% affected area showed  $>80\%$  or 60-80% yield  
488 reduction. The proportion of high yield reduction classes were found to be reduced as the  
489 proportion of affected area decrease. The GPs with  $<10\%$  affected area was found to be

490 dominated by the yield reduction class of <20%. In nutshell, the yield reduction of potato crop  
491 was corroborating well with the % of damage area at GP level. The result could have been  
492 improved further by the well distributed sampling procedure to address the local variations.

493 [Insert Figure 15](#)

#### 494 **4 Conclusions**

495 The present study demonstrated the potential of multi-temporal satellite data for objective  
496 assessment of potato crop area affected by hailstorm (25-28 February, 2019) in Hooghly and  
497 West Medinipur district of West Bengal. Extensive field information, collected over the potato  
498 crop before and after the event, revealed that the hailstorm caused significant damage by  
499 defoliating the crop canopy and increasing the soil wetness. Pre-event cloud free Sentinel-2  
500 data of 19<sup>th</sup> February along with the ground information were used to map the potato crop of  
501 affected districts with over all accuracy of 82%. This potato crop map was further used to assess  
502 the response of different band-reflectance of Sentinel-2 at pre-event and post-event condition.  
503 The NIR-reflectance was found to be highly sensitive to the changes in the canopy structure  
504 and surface wetness due to hailstorm. Red and SWIR bands were also showed sensitivity  
505 towards it. To accommodate the response of multiple bands towards damage of the crop, four  
506 different normalized vegetation indices (NDVI, NDWI, LSWI and NDTI) were derived using  
507 combinations of Red, NIR, SWIR1 and SWIR2 bands. All these indices showed high sensitivity  
508 and could able to separate different damage severity classes of potato crop. Based on the least  
509 co-linearity among these indices, NDVI and NDTI were selected to map the affected area.  
510 Decision matrix was prepared using the percentage change (pre- and post-event) of NDVI and  
511 NDTI over the different damage severity classes and further used it to map the potato crop area  
512 into “unaffected”, “moderately affected” and “severely affected” by hailstorm. Overall  
513 accuracy of the affected area map was found to be 86.7%. GP-wise yield reduction of potato

514 crop based on the CCE data were also found to be corroborating with the % of the area affected  
515 due to the hailstorm. Geospatial map of GP level affected potato crop area was also prepared to  
516 facilitate informed decision making. The study has thus established as scientific basis to  
517 objectively assess potato crop area affected due to hailstorm. Such value-added products would  
518 be very helpful in relief management and crop insurance value chain. Future study may be  
519 extended towards assessment of quantitative impact of hailstorm on the yield of potato crop.

## 520 **Acknowledgements**

521 Authors thankful to Director, NRSC, Hyderabad, India and Deputy Director, Remote Sensing  
522 Applications, NRSC for providing constant encouragement and facility to carry out the work.

## 523 **Declarations**

524 **Funding:** Not applicable.

525 **Conflicts of interest:** Authors have not reported any conflict of interest.

526 **Availability of data and material:** The satellite data that support the findings of this study  
527 are openly available at <https://www.copernicus.eu/en/access-data>. Other datasets are provided  
528 in the manuscript.

## 529 **References**

- 530 Apan A, Chandler O, Young FR and Maraseni TN (2005) Opportunities and limitations of  
531 remote sensing for crop loss (hail damage) assessment in the insurance industry.  
532 In *Proceedings of the 2005 Spatial Sciences Institute Biennial Conference 2005: Spatial*  
533 *Intelligence, Innovation and Praxis (SSC2005)* p. 19-28.
- 534 Bal SK, Saha S, Fand BB, Singh NP, Rane J, Minhas PS (2014) Hailstorms: Causes, Damage  
535 and Post-hail Management in Agriculture. Technical Bulletin No. 5, National Institute  
536 of Abiotic Stress Management, Malegaon, Baramati. 413 115.Pune, Maharashtra  
537 (India). p. 44. <http://dx.doi.org/10.13140/2.1.4841.7922>

538 Bal SK, Minhas PS, Singh Y, Kumar M, Patel DP, Rane J, Kumar PS, Ratnakumar P,  
539 Choudhury BU, Singh NP (2017) Coping with hailstorm in vulnerable Deccan Plateau  
540 region of India: technological interventions for crop recovery. *Curr Sci* 25:2021-7.  
541 <http://dx.doi.org/10.18520/cs/v113/i10/2021-2027>

542 Bell JR, Gebremichael E, Molthan AL, Schultz LA, Meyer FJ, Hain CR, Shrestha S, Payne KC  
543 (2020) Complementing optical remote sensing with synthetic aperture radar  
544 observations of hail damage swaths to agricultural crops in the central United States.  
545 *Journal of Applied Meteorology and Climatology*. 59(4):665-85.  
546 <https://doi.org/10.1175/JAMC-D-19-0124.1>

547 Bentley ML, Mote TL, Thebpanya P (2002) Using Landsat to identify thunderstorm damage in  
548 agricultural regions. *Bull Amer Meteor Soc* 83(3):363-76.  
549 <https://doi.org/10.1175/1520-0477-83.3.363>

550 Bidgoli RD, Koohbanani H, Keshavarzi A, Kumar V (2020) Measurement and zonation of soil  
551 surface moisture in arid and semi-arid regions using Landsat 8 images. *Arabian J Geosci*  
552 13(17):1-0. <https://doi.org/10.1007/s12517-020-05837-2>

553 Chandler O, Apan A, Pullinger R, Bullen K (2003) Quantifying hail damage for crop loss  
554 assessment: techniques using remote sensing and geographic information systems.  
555 In *Proceedings of the 11th Australasian Remote Sensing and Photogrammetry*  
556 *Conference* (ARSPC 2002), p. 412-421.  
557 <https://www.rocq.inria.fr/clime/lynx/chandler.pdf>

558 Changnon Jr SA (1971) Hailfall characteristics related to crop damage. *J Appl*  
559 *Meteorol* 10(2):270-274. <https://www.jstor.org/stable/26174912>

560 Changnon SA, Barron NA (1971) Quantification of crop-hail losses by aerial photography. *J*  
561 *Applied Meteorol and Climato* 10(1):86-96. [https://doi.org/10.1175/1520-0450\(1971\)010%3C0086:QOCHLB%3E2.0.CO;2](https://doi.org/10.1175/1520-0450(1971)010%3C0086:QOCHLB%3E2.0.CO;2)

562

563 Chattopadhyay N, Devi SS, John G, Choudhari VR (2017) Occurrence of hail storms and  
564 strategies to minimize its effect on crops. *Mausam* 68(1):75-92.

565 De US, Dube RK, Rao GP (2005) Extreme weather events over India in the last 100 years. *J.*  
566 *Ind Geophys Union* 9(3):173-87.

567 DACFW (2020) Department of Agriculture, Cooperation & Farmers Welfare. Directorate of  
568 Horticulture Government of India report available on  
569 <https://agricoop.nic.in/sites/default/files/Monthly%20Report%20on%20Potato%20for%20June%2C%202020.pdf>  
570

571 Drusch M, Del Bello U, Carlier S, Colin O, Fernandez V, Gascon F, Hoersch B, Isola C,  
572 Laberinti P, Martimort P, et al. (2012) Sentinel-2: ESA's optical high-resolution mission  
573 for GMES operational services. *Remote Sens Environ* 120:25-36.  
574 <https://doi.org/10.1016/j.rse.2011.11.026>

575 Erickson BJ, Johannsen CJ, Vorst JJ, Biehl LL (2004) Using remote sensing to assess stand  
576 loss and defoliation in maize. *Photogramm Eng Remote Sens* 70(6):717-22.  
577 <http://dx.doi.org/10.14358/PERS.70.6.717>

578 Gallo K, Smith T, Jungbluth K, Schumacher P (2012) Hail swaths observed from satellite data  
579 and their relation to radar and surface-based observations: A case study from Iowa in  
580 2009. *Weather and forecasting* 27(3):796-802. [https://doi.org/10.1175/WAF-D-11-](https://doi.org/10.1175/WAF-D-11-00118.1)  
581 [00118.1](https://doi.org/10.1175/WAF-D-11-00118.1)

582 Games PA, Howell JF (1976) Pairwise multiple comparison procedures with unequal n's and/or  
583 variances: a Monte Carlo study. *J Educational Statistics* 1(2):113-25.  
584 <https://doi.org/10.2307/1164979>

585 Gao BC (1996) NDWI-A normalized difference water index for remote sensing of vegetation  
586 liquid water from space. *Remote Sens Environ* 58(3):257-66.  
587 [https://doi.org/10.1016/S0034-4257\(96\)00067-3](https://doi.org/10.1016/S0034-4257(96)00067-3)

588 Gillis MD, Leckie DG, Pick RD (1990) Satellite imagery assists in the assessment of hail  
589 damage for salvage harvest. *The Forestry Chronicle*. 66(5):463-8.  
590 <https://doi.org/10.5558/tfc66463-5>

591 Glance, HSAA (2018) Horticulture Statistics Division Department of Agriculture. Cooperation  
592 & Farmers' Welfare Ministry of Agriculture and Farmers' Welfare Government of India.  
593 [https://agricoop.nic.in/sites/default/files/Horticulture%20Statistics%20at%20a%20Gla](https://agricoop.nic.in/sites/default/files/Horticulture%20Statistics%20at%20a%20Glance-2018.pdf)  
594 [nce-2018.pdf](https://agricoop.nic.in/sites/default/files/Horticulture%20Statistics%20at%20a%20Glance-2018.pdf)

595 Gorelick N, Hancher M, Dixon M, Ilyushchenko S, Thau D, Moore R (2017) Google Earth  
596 Engine: Planetary-scale geospatial analysis for everyone. *Remote Sens Environ* 202:18-  
597 27. <https://doi.org/10.1016/j.rse.2017.06.031>

598 Hunt Jr ER, Rock BN (1989) Detection of changes in leaf water content using near-and middle-  
599 infrared reflectances. *Remote Sens Environ* 30(1):43-54. [https://doi.org/10.1016/0034-](https://doi.org/10.1016/0034-4257(89)90046-1)  
600 [4257\(89\)90046-1](https://doi.org/10.1016/0034-4257(89)90046-1)

601 ICAR (2017) West Bengal Agriculture Contingency Plan for District: Paschim Medinipur.  
602 <http://krishi.icar.gov.in/jspui/handle/123456789/29255>

603 Irigoyen I, Domeño I, Muro J (2011) Effect of defoliation by simulated hail damage on yield  
604 of potato cultivars with different maturity performed in Spain. *American J Potato Res*  
605 88(1):82-90. <http://dx.doi.org/10.1007/s12230-010-9166-z>

606 Jalali AH (2013) Potato (*Solanum tuberosum* L.) yield response to simulated hail  
607 damage. *Archives Agronomy Soil Sci* 59(7): 981-987.  
608 <http://dx.doi.org/10.2134/agronj2004.0283>

609 Klimowski BA, Hjelmfelt MR, Bunkers MJ, Sedlacek D, Johnson LR (1998) Hailstorm damage  
610 observed from the GOES-8 satellite: The 5–6 July 1996 Butte–Meade storm. *Mon*  
611 *Weather Rev* 126(3):831-4. [https://doi.org/10.1175/1520-0493\(1998\)126%3C0831:HDOFTG%3E2.0.CO;2](https://doi.org/10.1175/1520-0493(1998)126%3C0831:HDOFTG%3E2.0.CO;2)

613 Kulkarni JR, Morwal SB, Narkhedkar SG, Maheskumar RS, Padmakumari B, Sunitha Devi S,  
614 Rajeevan M (2015) Unprecedented hailstorms over north peninsular India during  
615 February–March 2014. *J Geophys Res: Atmospheres* 120(7):2899-912.  
616 <https://doi.org/10.1002/2015JD023093>

617 Kumar P, Gupta DK, Mishra VN, Prasad R (2015) Comparison of support vector machine,  
618 artificial neural network, and spectral angle mapper algorithms for crop classification  
619 using LISS IV data. *Intern J Remote Sens* 36(6):1604-17.  
620 <https://doi.org/10.1080/2150704X.2015.1019015>

621 Matirkatha (2016) <http://matirkatha.net/wp-content/uploads/2016/07/Land-Use-Statistics.pdf>

622 Mohanty A (2020) Preparing India for Extreme Climate Events: Mapping Hotspots and  
623 Response Mechanisms, New Delhi: Council on Energy, Environment and Water  
624 [https://www.ceew.in/sites/default/files/CEEW-Preparing-India-for-extreme-climate-  
625 events\\_10Dec20.pdf](https://www.ceew.in/sites/default/files/CEEW-Preparing-India-for-extreme-climate-events_10Dec20.pdf)

626 Moran MS, Inoue Y, Barnes EM (1997) Opportunities and limitations for image-based remote  
627 sensing in precision crop management. *Remote Sens Environ* 61(3):319-46.  
628 [https://doi.org/10.1016/S0034-4257\(97\)00045-X](https://doi.org/10.1016/S0034-4257(97)00045-X)

629 Nagar BL, Yadav DL, Baldev R, Narolia RS (2019) Performance of potato varieties for growth,  
630 yield and yield attributing in South Eastern Rajasthan. *J Experiment Bio Agric Sci*  
631 7(5):438-41. [http://dx.doi.org/10.18006/2019.7\(5\).438.441](http://dx.doi.org/10.18006/2019.7(5).438.441)

632 NIE (2019) [https://www.newindianexpress.com/nation/2019/feb/25/seasons-first-norwester-  
633 claims-4-lives-in-west-bengal-1943531.html](https://www.newindianexpress.com/nation/2019/feb/25/seasons-first-norwester-claims-4-lives-in-west-bengal-1943531.html) (visited 28.07.2021)

634 NRSC (2014) Land Use/Land Cover Database on 1:50,000 Scale. Natural Resources Census  
635 Project. Hyderabad: LUCMD, LRUMG, RSAA, National Remote Sensing Centre,  
636 ISRO.

637 Parihar JS, Oza MP, Parihar JS, Saito G (2006) FASAL: an integrated approach for crop  
638 assessment and production forecasting. In Agriculture and hydrology applications of  
639 remote sensing. Vol. 6411, p. 641101. International Society for Optics and Photonics.  
640 <http://dx.doi.org/10.1117/12.713157>

641 Parker MD, Ratcliffe IC, Henebry GM (2005) The July 2003 Dakota hail swaths: Creation,  
642 characteristics, and possible impacts. Mon Wea Rev 133(5):1241-60.  
643 <https://doi.org/10.1175/MWR2914.1>

644 Peters AJ, Griffin SC, Viña A, Ji L (2000) Use of remotely sensed data for assessing crop hail  
645 damage. PE&RS, Photogramm Eng Remote Sens 66(11):1349-55.

646 PMFBY (2020) Pradhan Mantri Fasal Bima Yojana: Revamped Operational Guidelines  
647 Pradhan Mantri Fasal Bima Yojana (Effective from Kharif 2020), Department of  
648 Agriculture, Cooperation and Farmers Welfare Ministry of Agriculture & Farmers  
649 Welfare Government of India, File Number - 13015/03/2018-Credit II.  
650 [https://www.pmfby.gov.in/pdf/Revamped%20Operational%20Guidelines\\_17th%20A  
651 ugust%202020.pdf](https://www.pmfby.gov.in/pdf/Revamped%20Operational%20Guidelines_17th%20August%202020.pdf)

652 Prabhakar M, Gopinath KA, Reddy AG, Thirupathi M, Rao CS (2019) Mapping hailstorm  
653 damaged crop area using multispectral satellite data. The Egyptian J Remote Sens Space  
654 Sci 22(1):73-9. <https://doi.org/10.1016/j.ejrs.2018.09.001>

655 Quemada M, Daughtry CS (2016) Spectral indices to improve crop residue cover estimation  
656 under varying moisture conditions. Remote Sens 8(8):660.  
657 <https://doi.org/10.3390/rs8080660>

658 Rao VUM, Rao BB, Sikka AK, Rao AS, Singh R, Maheswari M (2014) Hailstorm Threat to  
659 Indian Agriculture: A Historical Perspective and Future Strategies, Hyderabad-500 059:  
660 44.  
661 <http://www.cropweatheroutlook.in/crida/amis/Hailstorm%20Technical%20bulletin.pdf>

662 Ray SS, Singh SK, Mamatha S (2016) Establishing an operational system for assessment and  
663 forecasting the impact of extreme weather events on crop production. Mausam  
664 67(1):289-96.

665 Renier C, Waldner F, Jacques DC, Babah Ebbe MA, Cressman K, Defourny P (2015) A  
666 dynamic vegetation senescence indicator for near-real-time desert locust habitat

667 monitoring with MODIS. Remote Sens 7(6):7545-70.  
668 <https://doi.org/10.3390/rs70607545>

669 Rouse JW, Haas RH, Schell JA, Deering DW (1974) Monitoring Vegetation Systems in the  
670 Great Plains with ERTS. Proceedings, 3rd Earth Resource Technology Satellite (ERTS)  
671 Symposium 1:48-62. <https://ntrs.nasa.gov/citations/19740022614>.

672 Singh SK, Saxena R, Porwal A, Ray N, Ray SS (2017) Assessment of hailstorm damage in  
673 wheat crop using remote sensing. Current Sci 112(10):2095-100.  
674 <http://dx.doi.org/10.18520/cs/v112/i10/2095-2100>

675 Tiwari JK, Singh B, Bhardwaj V, Singh RK, Pandey NK, Chakrabarti SK, Kumar M (2021)  
676 Impact of ICAR-CPRI Technologies on Potato in India, eTechnical Bulletin No. 5 Ref.:  
677 No.F.PME/3-3/2021 dated 4.7.2021.  
678 <https://cpri.icar.gov.in/WriteReadData/LINKS/Impact%20CPRI%20tech%20on%20potato%20in%20India%208-7-21da1f3f68-ceb3-43ed-be21-ea4a7d2346fd.pdf> accessed  
679 on 28th July, 2021

680

681 Towery NG (1980) Some Applications of Remote Sensing of Crop-Hail Damage in the  
682 Insurance Industry; Circular 143/80 of the Illinois State Water Survey, Illinois Institute  
683 of Natural Resources: Urbana, IL, USA, 1980; p. 17. <http://hdl.handle.net/2142/94454>

684 Towery NG, Eyton JR, Changnon Jr SA, Dailey CL (1975) Remote sensing of crop hail  
685 damage. Illinois State Water Survey. Report of Research Conducted for the country  
686 companies. P. 29.  
687 [https://www.ideals.illinois.edu/bitstream/handle/2142/55723/ISWSCR-](https://www.ideals.illinois.edu/bitstream/handle/2142/55723/ISWSCR-165.pdf?sequence=2)  
688 [165.pdf?sequence=2](https://www.ideals.illinois.edu/bitstream/handle/2142/55723/ISWSCR-165.pdf?sequence=2)

689 Van Deventer AP, Ward AD, Gowda PH, Lyon JG (1997) Using thematic mapper data to  
690 identify contrasting soil plains and tillage practices. Photogramm Eng Remote Sens  
691 63:87-93.

692 Weather (2019) [https://weather.com/en-IN/india/news/news/2019-02-26-thunder-and-hail-](https://weather.com/en-IN/india/news/news/2019-02-26-thunder-and-hail-across-kolkata-and-south-bengal)  
693 [across-kolkata-and-south-bengal](https://weather.com/en-IN/india/news/news/2019-02-26-thunder-and-hail-across-kolkata-and-south-bengal) (visited 28.07.2021)

694 Xue J, Su B (2017) Significant remote sensing vegetation indices: A review of developments  
695 and applications. J sensors <https://doi.org/10.1155/2017/1353691>

696 Zhao JL, Zhang DY, Luo JH, Huang SL, Dong YY, Huang WJ (2012) Detection and mapping  
697 of hail damage to corn using domestic remotely sensed data in China. Australian J Crop  
698 Sci 6(1):101-8.

699 Zhou J, Pavek MJ, Shelton SC, Holden ZJ, Sankaran S (2016) Aerial multispectral imaging for  
700 crop hail damage assessment in potato. *Computer Electronics Agric* 127:406-12.  
701 <http://dx.doi.org/10.1016/j.compag.2016.06.019>

702 Zhou Y, Liu H, He B, Yang X, Feng Q, Kutser T, Chen F, Zhou X, Xiao F, Kou J (2021) Secchi  
703 Depth estimation for optically-complex waters based on spectral angle mapping-derived  
704 water classification using Sentinel-2 data. *Inter J Remote Sens* 42(8):3123-45.  
705 <https://doi.org/10.1080/01431161.2020.1868606>

706  
707  
708  
709  
710  
711  
712  
713  
714  
715  
716  
717  
718

719  
720  
721  
722  
723  
724  
725  
726  
727  
728  
729  
730  
731  
732  
733  
734  
735  
736  
737  
738  
739  
740  
741  
742  
743  
744  
745  
746  
747  
748  
749  
750  
751

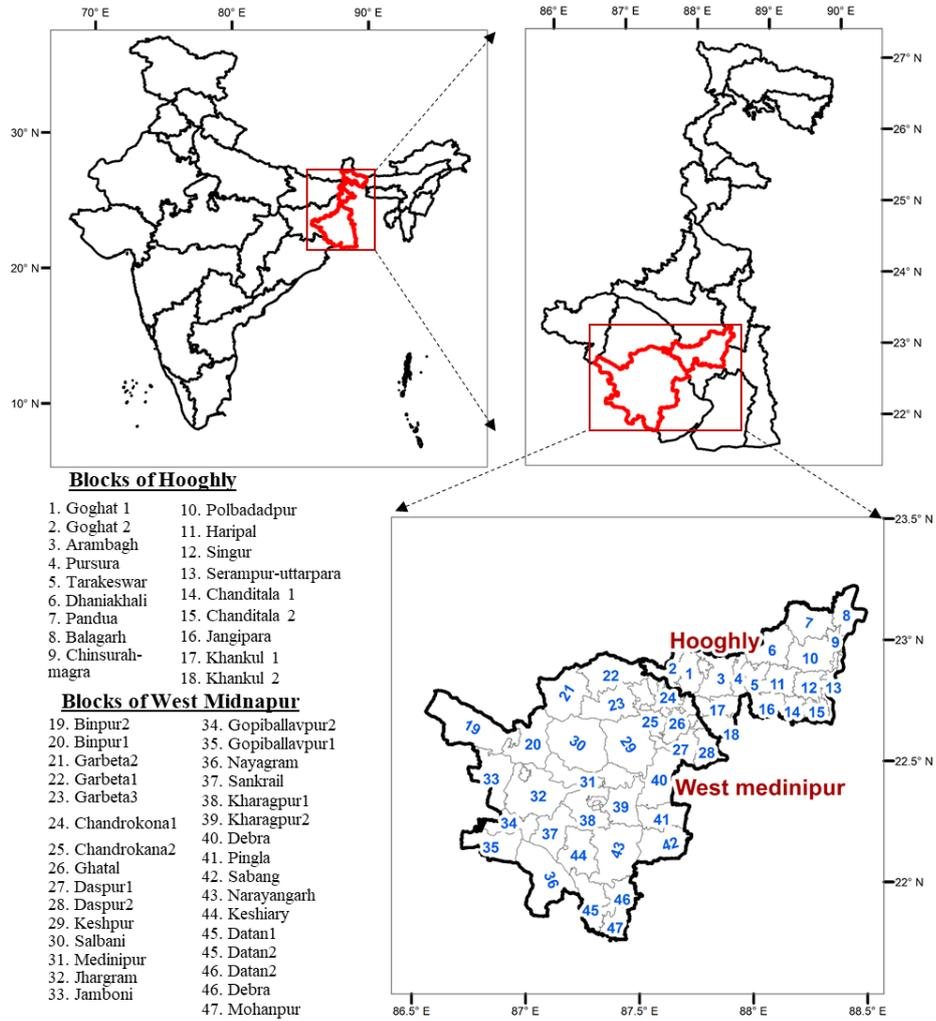
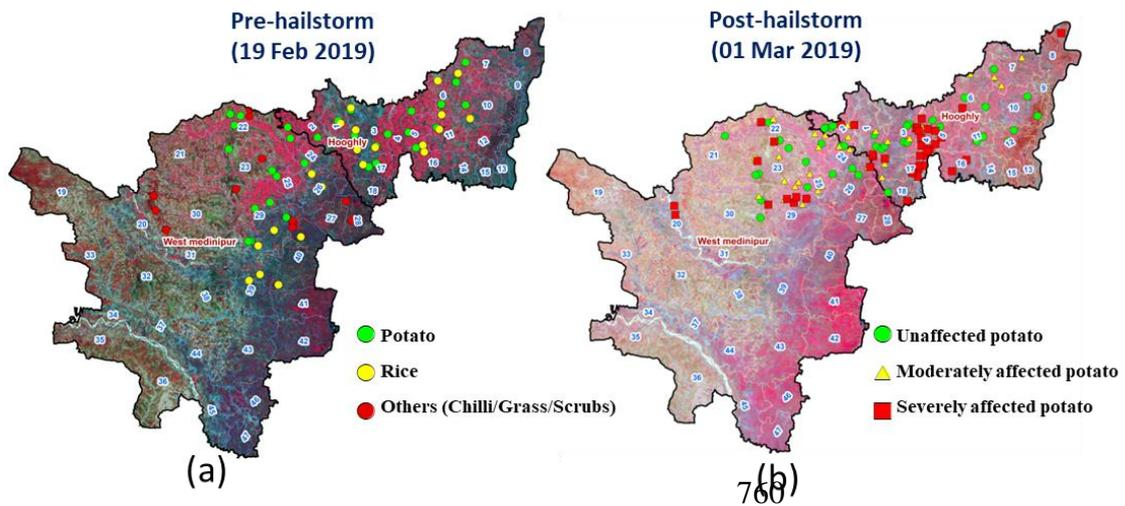


Fig 1 Location of the study area

752



761

762 Fig 2 Ground truth points overlaid on Sentinel-2 false colour composites (R:G:B = B8:B4:B3)

763 (a) Pre-event & (b) Post-event.

764

765

766

767

768

769

770

771

772

773

774

775

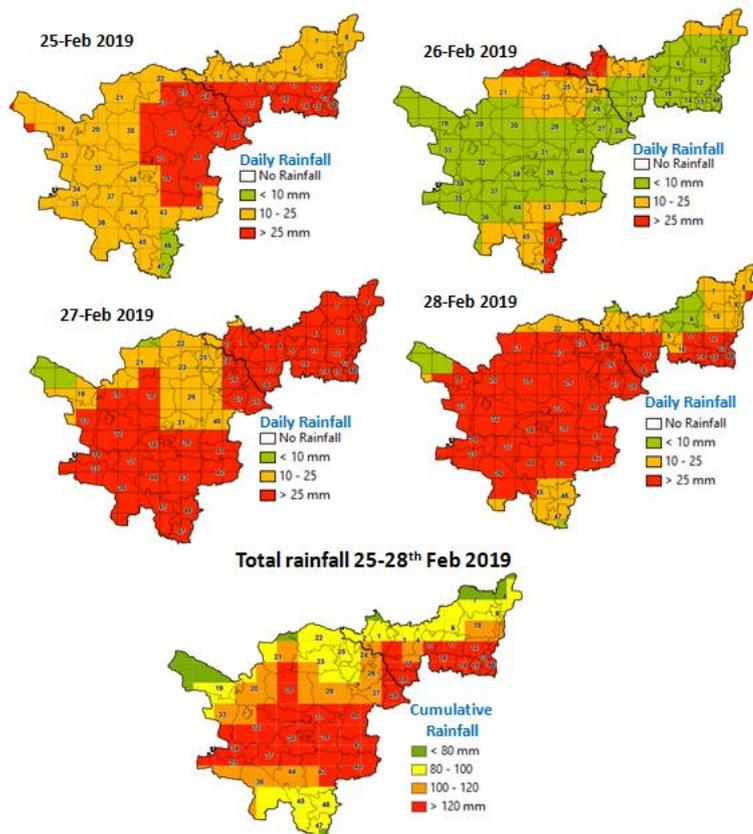
776

777

778

779

780



781 Fig 3 Rainfall over Hooghly and West Medinipur districts of West Bengal during 25-28

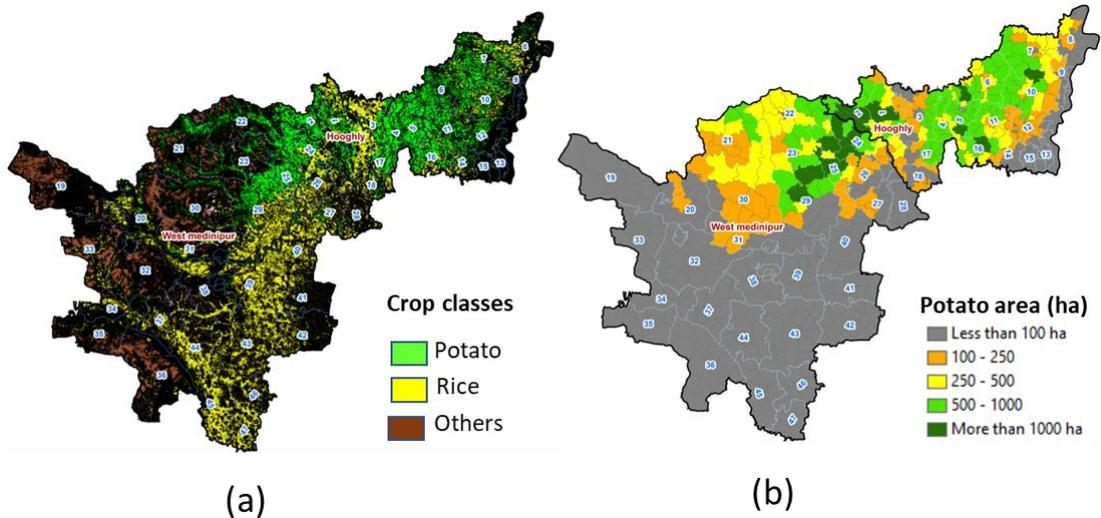
782 February 2019 as represented by 0.1° X 0.1° rainfall by IMD

783  
784  
785  
786  
787  
788  
789  
790  
791  
792  
793



794 Fig 4 Field photographs showing severity of damage of the potato crop in the study area due to  
795 hailstorm

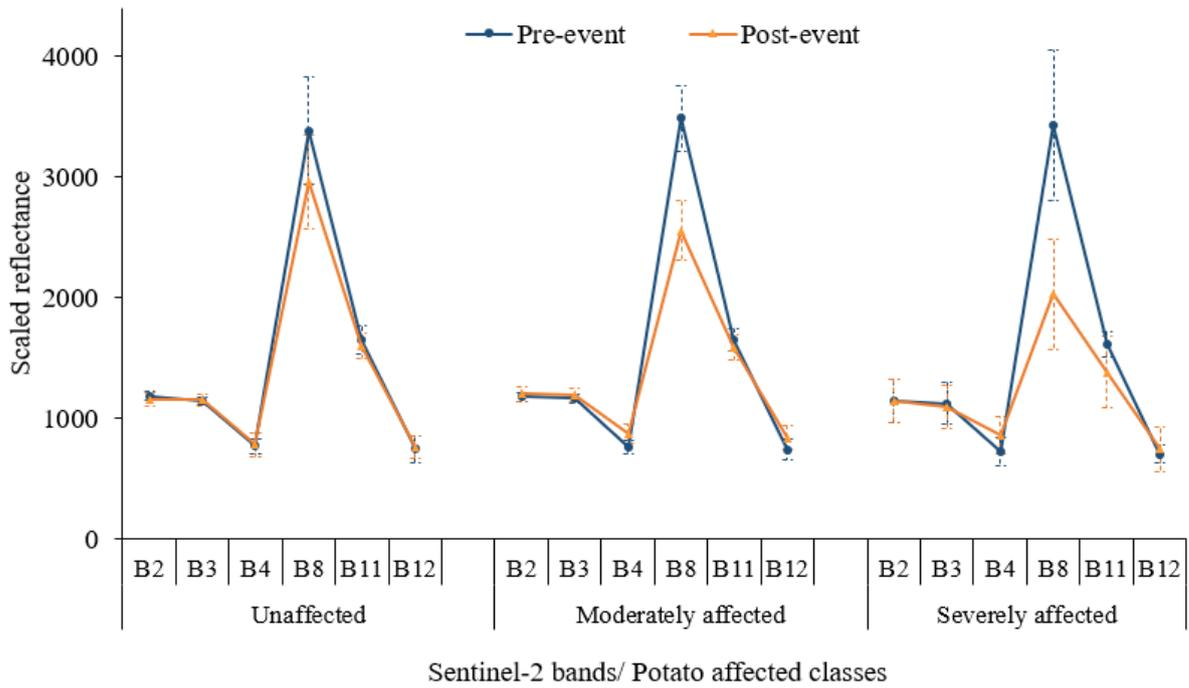
796  
797  
798  
799  
800  
801  
802  
803  
804  
805  
806



807

808 Fig 5 (a) Classified crop map of the study area as on 19<sup>th</sup> Feb 2019; (b) GP wise area under  
809 potato crop

810  
811  
812  
813  
814



816 Fig 6 Reflectance of selected bands of Sentinel-2 over the different damage severity classes of  
 817 potato crop before (19<sup>th</sup> February) and after (1<sup>st</sup> March) the hailstorm. Standard deviations are  
 818 represented as error bars.

819

820

821

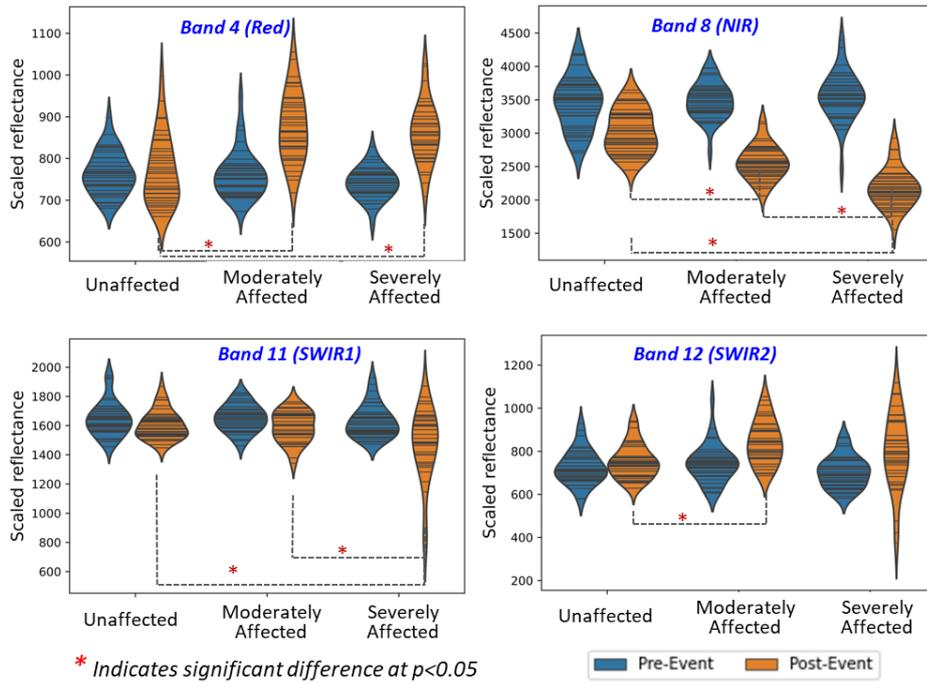
822

823

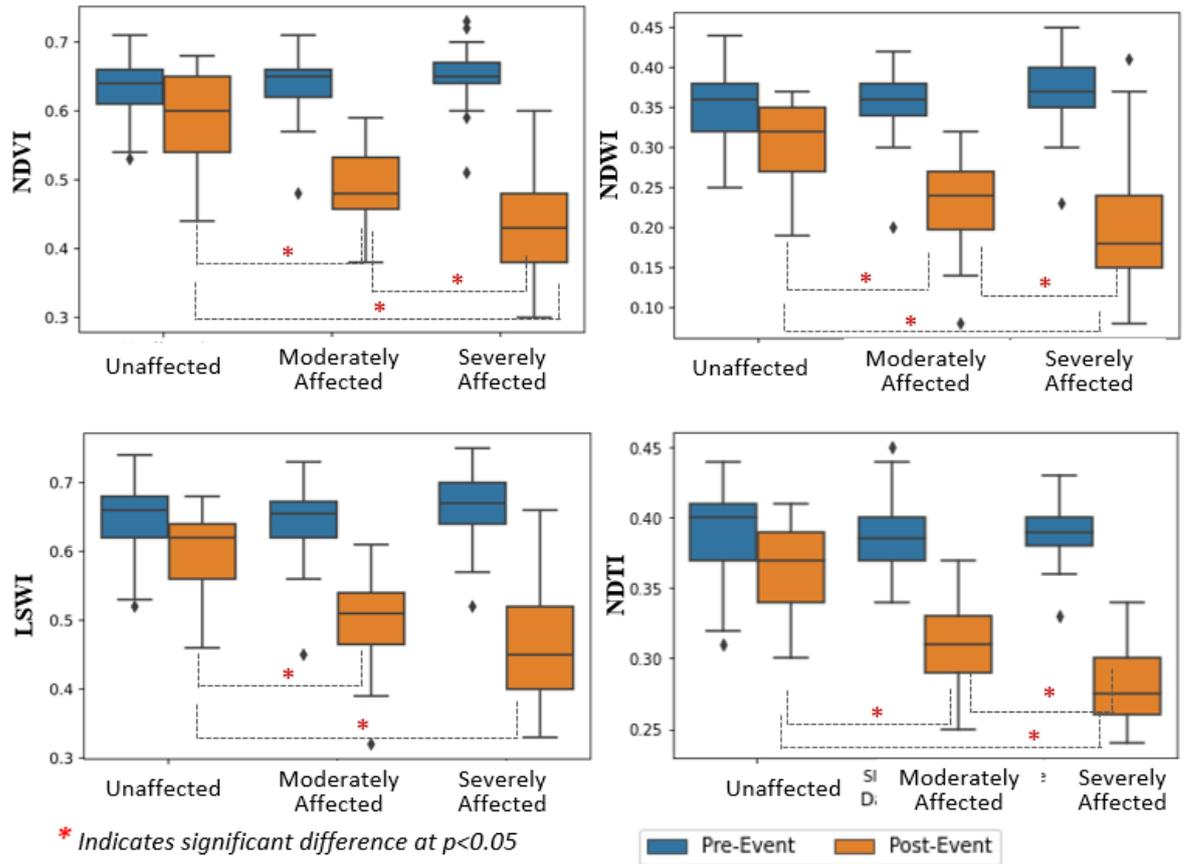
824

825

826  
827  
828  
829  
830  
831  
832  
833  
834  
835  
836  
837  
838



839 Fig 7 Violin-plot showing the data distribution of the band-reflectance (pre- and post-event)  
840 over the different damage severity classes of potato crops due to hailstorm. The band  
841 observations significantly (Post-hoc Games-Howell tests) different over the different severity  
842 classes are mentioned as \*.  
843



844

845 Fig 8 Box-plot showing the variations of different normalized-indices (pre and post-event) over  
 846 the different damage severity classes of potato crops due to hailstorm. The normalized-indices  
 847 significantly (Post-hoc Games-Howell tests) different over the different severity classes are  
 848 mentioned as \*.

849

850

851

852

853

854

855

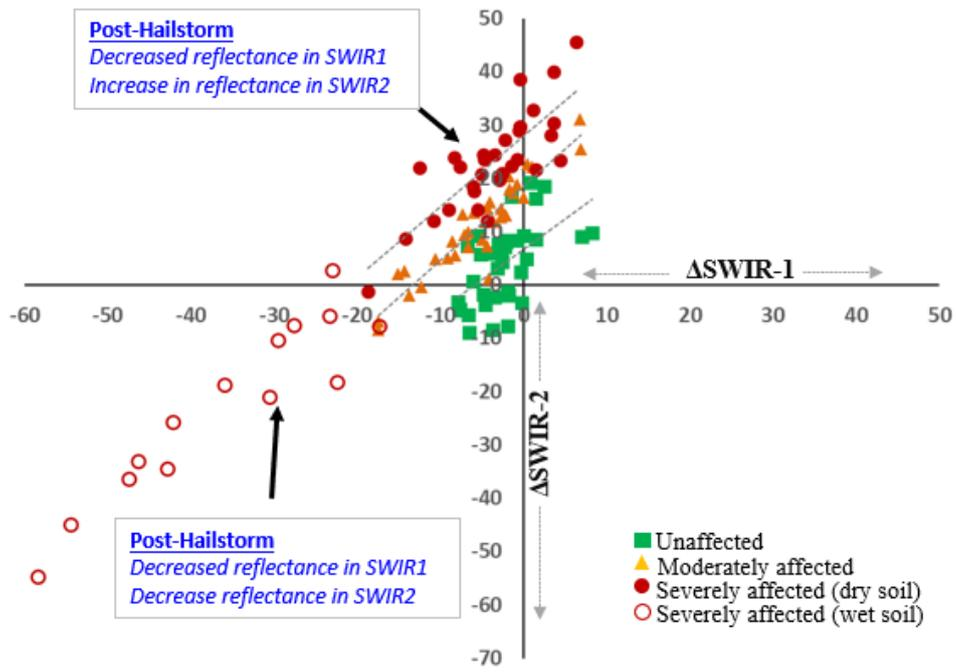
856

857

858

859

860



013

874 Fig 9 Scatterplot of  $\Delta$ SWIR-1 and  $\Delta$ SWIR-2 showing separability of the different damage  
 875 severity classes of the potato crop

876

877

878

879

880

881

882

883

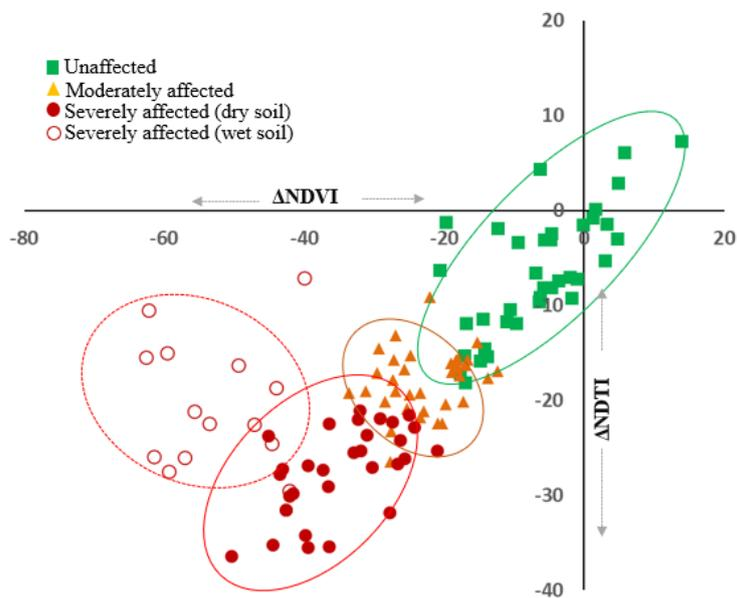
884

885

886

887

888

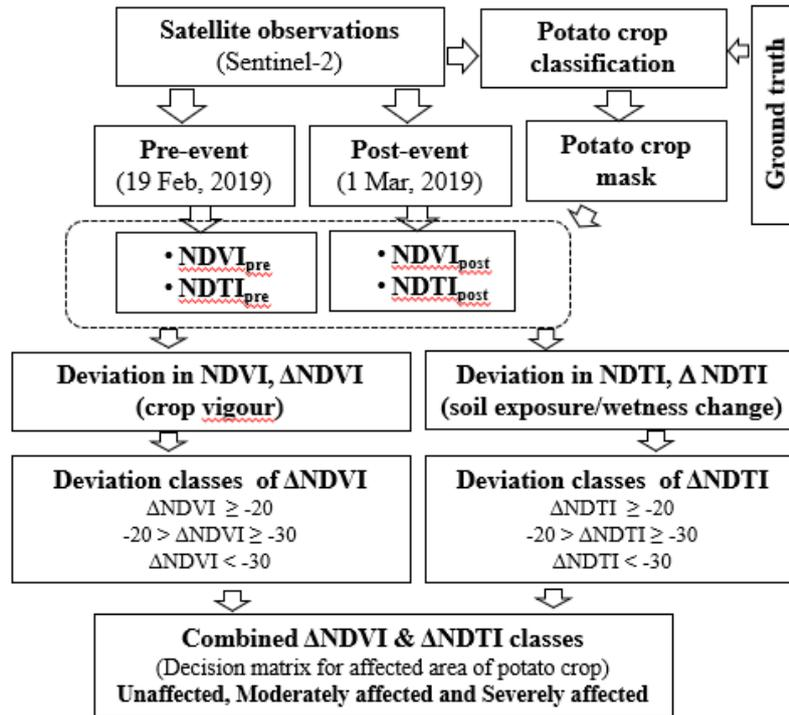


889 Fig 10 Scatterplot of  $\Delta$ NDVI and  $\Delta$ NDTI showing separability of the different damage severity  
 890 classes of the potato crop.

891

892

893  
894  
895  
896  
897



905  
906

Fig 11 Schematic diagram of the proposed methodology

**Increase in soil exposure/wetness change  
( $\Delta$ NDTI)**

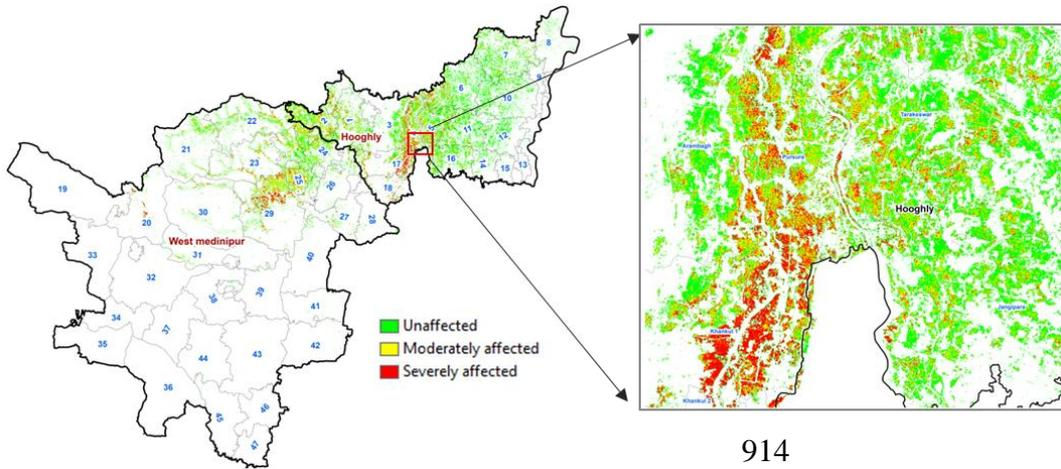
	$\geq -20\%$	-20 to -30%	$< -30\%$
$\geq -20\%$	Unaffected	Moderate	NE
-20 to -30%	Moderate	Moderate	Severe
$< -30\%$	Severe	Severe	Severe

\*NE: Non-existent

907  
908  
909  
910  
911  
912

Fig 12 Decision matrix of different categories of affected area based on  $\Delta$ NDVI and  $\Delta$ NDTI

913



915 Fig 13 Spatial distribution of the different categories of potato crop affected due to hail storm  
916 over Hooghly and West-Medinipur district

917

918

919

920

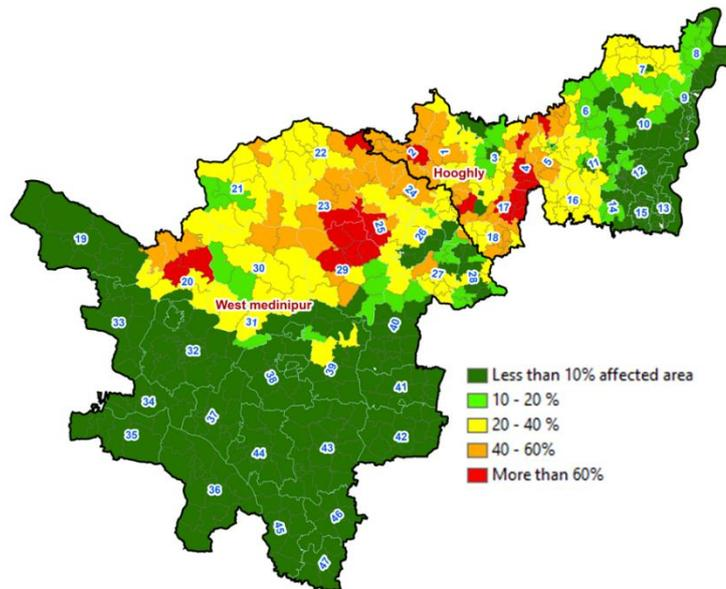
921

922

923

924

925



926 Fig 14 GP-wise percentage of potato crop affected (both moderately and severely) due to  
927 hailstorm over Hooghly and West Medinipur

928

929

930

931

932

933

934  
935  
936  
937  
938  
939  
940  
941  
942  
943  
944  
945  
946  
947  
948  
949  
950  
951  
952  
953  
954  
955  
956  
957  
958  
959

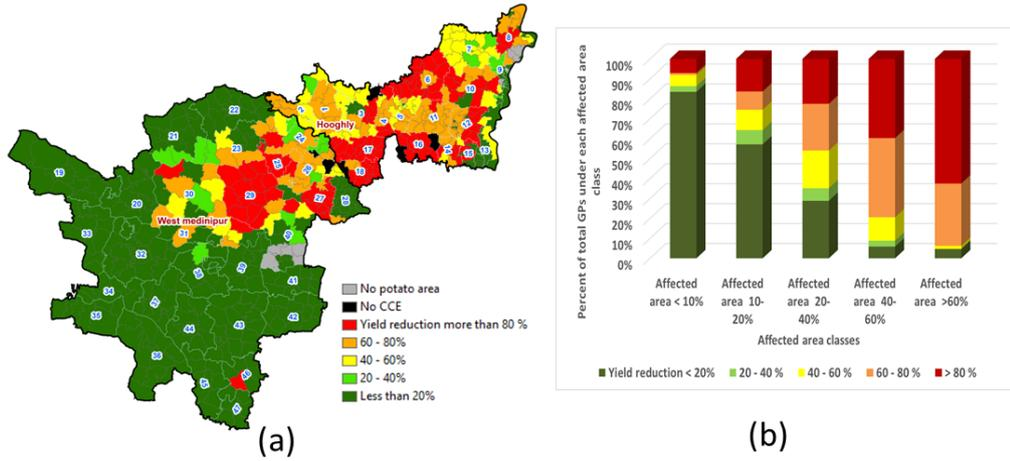


Fig 15 (a) GP wise potato yield reduction in 2019 as compared to historical six years (b) Distribution of GPs into different yield reduction classes under each affected area classes

960

Table 1 Detailed specification of the Sentinel-2 data used in the present study

Spectral Bands	Central wavelength (μm)	Spatial resolution(m)
B2 - Blue	0.490	10
B3 - Green	0.560	10
B4 - Red	0.665	10
B8 - NIR	0.842	10
B11 – SWIR 1	1.610	20
B12 – SWIR 2	2.190	20

961

962

963

964

965

966 Table 2 Vegetation indices used in the study

Vegetation Indices	Formula	Significance	Reference
NDVI	$\frac{B8 - B4}{B8 + B4}$	<ul style="list-style-type: none"> <li>• Sensitive to green vegetation</li> <li>• Influenced by leaf chlorophyll and moisture</li> <li>• Represents photosynthetic vegetation fraction</li> </ul>	Rouse et al. 1974
NDWI	$\frac{B8 - B11}{B8 + B11}$	<ul style="list-style-type: none"> <li>• Sensitive to canopy moisture</li> <li>• Influenced by leaf structure and wetness</li> </ul>	Gao, 1996
LSWI	$\frac{B8 - B12}{B8 + B12}$	<ul style="list-style-type: none"> <li>• Sensitive to canopy and soil moisture</li> </ul>	Hunt and Rock 1989
NDTI	$\frac{B11 - B12}{B11 + B12}$	<ul style="list-style-type: none"> <li>• Sensitive to soil moisture and non-photosynthetic vegetation (NPV)</li> <li>• Do not influence much by leaf mesophyll cell structure</li> </ul>	Van Deventer et al. 1997

967

968

969

970

971

972

973

974

975

976 Table 3 Statistical analysis of the mean of percent change (from pre-event to post event) of  
 977 different band-reflectance and vegetation indices.

Severity classes	N	$\overline{\Delta Red}$	$\overline{\Delta NIR}$	$\overline{\Delta SWIR1}$	$\overline{\Delta SWIR2}$	$\overline{\Delta NDVI}$	$\overline{\Delta NDWI}$	$\overline{\Delta LSWI}$	$\overline{\Delta NDTI}$
Unaffected	37	0.82 <sup>a</sup>	<b>-11.73<sup>a</sup></b>	-2.40 <sup>a</sup>	3.92 <sup>a</sup>	<b>-6.55<sup>a</sup></b>	<b>-13.07<sup>a</sup></b>	<b>-7.58<sup>a</sup></b>	<b>-6.45<sup>a</sup></b>
Moderately affected	36	15.13 <sup>b</sup>	<b>-26.60<sup>b</sup></b>	-3.72 <sup>a</sup>	13.70 <sup>b</sup>	<b>-23.75<sup>b</sup></b>	<b>-35.47<sup>b</sup></b>	<b>-22.56<sup>b</sup></b>	<b>-19.02<sup>b</sup></b>
Severely affected	46	16.63 <sup>b</sup>	<b>-38.56<sup>c</sup></b>	-10.13 <sup>b</sup>	12.80 <sup>bc</sup>	<b>-34.20<sup>c</sup></b>	<b>-46.80<sup>c</sup></b>	<b>-30.10<sup>c</sup></b>	<b>-24.35<sup>c</sup></b>
Variance analysis	F-value	28.0	194.1	16.5	3.6	106.1	44.4	61.4	86.2
	P	.000	.000	.000	.031	.000	.000	.000	.000

978 *N= no of samples. Letters in upper script (a-c) indicate significant difference at P<0.05*  
 979 *(Posthoc Games-Howell tests were performed for separation of means; means with at least one*  
 980 *letter common are not statistically significant). The mean values of the severity classes*  
 981 *statistically different from each other are mentioned as bold letters.*

982  
 983  
 984  
 985

986 Table 4 Correlation matrix between different vegetation indices at pre- and post-event of the  
 987 hailstorm.

<b>Pre-event</b>				
	NDVI	NDWI	LSWI	NDTI
NDVI	1			
NDWI	0.86	1		
LSWI	0.88	0.98	1	
NDTI	0.80	0.91	0.97	1
<b>Post-event</b>				
NDVI	1			
NDWI	0.87	1		
LSWI	0.83	0.99	1	
NDTI	0.78	0.90	0.96	1

997  
 998  
 999  
 1000

1001 Table: 5 Accuracy assessment table for potato damage area classes

1002

1003

1004

1005

Severity classes	Producer's accuracy	User's accuracy
Unaffected	92.7	90.0
Moderately affected	75.2	80.1
Severely affected	88.2	77.3